© 1999 The Chemical Society of Japan
Bull. Chem. Soc. Jpn., 72, 2261—2270 (1999)

Dioxomolybdenum(VI) and Dioxotungsten(VI) Structure with Mono(Dithiolato) Coordination: Crystal Structures, Properties and Reactivity of $[\{M^{VI}O_2(dithiolato)\}_2(\mu\text{-}O)]^{2-}$ (M = Mo and W) Complexes

Hiroyuki Oku,# Norikazu Ueyama, and Akira Nakamura*

Department of Macromolecular Science, Graduate School of Science, Osaka University, Toyonaka, Osaka 560-0043

(Received June 2, 1999)

Novel mono(dithiolato) molybdenum(VI) and tungsten(VI) complexes were isolated through the searching for potential active species in the catalytic air oxidation of benzoin by $[Mo^{V}O(SR)_4]^-$ complexes. Among these, $(NEt_4)_2[\{Mo^{VI}O_2$(3-triphenylsilyl-1,2-benzenedithiolato)$\}_2(\mu$-O)]·2DMF (**1**), $(PPh_4)_2[\{W^{VI}O_2$(1,2-benzenedithiolato)$\}_2(\mu$-O)] (**3**), and $(NEt_4)_2[\{W^{VI}O_2$(2,3-naphthalenedithiolato)$\}_2(\mu$-O)] (**5**) were structurally characterized by X-ray crystallography. The electrochemical, electronic, as well as Raman/IR spectral properties of the tungsten complexes, **3** and **5**, have been investigated and compared with the corresponding bis(dithiolato) complexes, e.g. $[W^{VI}O_2(dithiolato)_2]^{2-}$. The μ-oxo-binuclear species, $[\{Mo^{VI}O_2(SR)_2\}_2(\mu\text{-}O)]^{2-}$, is proposed as a possible active species for the catalytic air oxidation of benzoin by the Mo(V) thiolato complexes.

Much attention has been paid to the coordination chemistry of oxo-molybdenum and -tungsten compounds having dithiolene ligands owing to their relevance for the active site structure of molybdenum and tungsten oxidoreductases. Based on the crystallographic studies, the memberes of the family of molybdenum oxidoreductases have been classified into two groups. One group has mono-coordination of pterin-dithiolene ligand (pterin cofactor) to a molybdenum ion, e.g. aldehyde oxidoreductase and xanthine oxidase.[1] The other group has bis-coordination of the dithiolene ligand, e.g. DMSO reductase.[2]

To reveal the structure and reactivity of the enzyme active site, dithiolene-molybdenum and -tungsten complexes have been extensively studied.[3—5] Among these complexes, some proceed the following oxo-transfer reaction (Eq. 1) where the substrate is reduced to X or oxidized to XO.[3,4b,5]

$$(M^{IV}O)^{2+} + XO \rightleftarrows (M^{VI}O_2)^{2+} + X \qquad (1)$$

As a study of the alcoholic C–H oxidation, benzoin has been frequently employed as a substrate.[3c,3d,5] The reaction proceeds as described in Eq. 2.

$$\text{benzoin} + XO \longrightarrow \text{benzil} + H_2O + X \qquad (2)$$

Our reactivity study showed that the tungsten thiolato complexes have almost the same activity as the corresponding molybdenum complex.[3c,3b] Actually for the aldehyde (R–CHO) oxidation, a benzoin-related compound, acetal ($R\text{–}CH(OH)_2$), is a probable reaction intermediate and also a substrate in both molybdenum and tungsten enzymes.[1,6] The other related substrate, a hydroxycarboxylate (= RCH(OH)-COO^-), is catalytically oxidized by a molybdenum enzyme isolated from *Proteus vulgaris* and *Proteus mirablis*.[7]

In the previous study, during the catalytic oxidation of benzoin with a reduced state enzyme model, $[Mo^{IV}O(bdt)_2]^{2-}$ (bdt = 1,2-benzenedithiolate), we have successfully prepared an oxidized state model complex, $[Mo^{VI}O_2(bdt)_2]^{2-}$ which has two dithiolene ligands.[3e,5c] This type of dioxomolybdenum(VI) complex has long been considered as unstable due to the strong *trans* influence between oxo and thiolate ligand.[8]

We have also studied the catalytic activity of a Mo(V) complex, $[Mo^{V}O(SR)_4]^-$, for the oxidation of benzoin by air.[5d] During the air oxidation study of Mo(V), we have found a complex which has mono(dithiolene) and *cis*-dioxo ligands coordinate to a Mo(VI) ion, although it is not a mononuclear Mo(VI) compound.[3f] In this paper we describe the crystal structures, properties, and reactivity of $[\{M^{VI}O_2$(dithiolato)$\}_2(\mu$-O)]$^{2-}$ (M = Mo and W, dithiolato = 1,2-benzenedithiolate (= bdt), 3-triphenylsilyl-1,2-benzenedithiolate (= Ph_3Si-bdt), and 2,3-naphthalenedithiolate (= ndt)) complexes.

Experimental

All operations except those mentioned were carried out under argon atmosphere. *N,N*-Dimethylformamide (DMF), diethyl ether, and dimethylsulfoxide (DMSO) were purified by distillation before use. Benzoin used was recrystallized from ethanol–diethyl ether. Due to the limitations of sample amount, we did not perform elemental analyses.

$(NEt_4)_2[\{Mo^{VI}O_2(Ph_3Si\text{-}bdt)\}_2(\mu\text{-}O)]$·2DMF (1). DMF solution (1 cm^3) of $(NEt_4)[Mo^{V}O(Ph_3Si\text{-}bdt)_2]$ (**2**)[3f] (5 mg, 5×10^{-3}

Present address: Department of Chemistry, Gunma University, Kiryu, Gunma 376-8515, Japan.

mmol) was prepared under Ar atmosphere. To this solution, diethyl ether (5 cm^3) vapor was diffused slowly during 40 d to precipitate crystals. During the crystal formation, a small amount of air was introduced through a small opening of the glass plug. Finally, almost all of **2** was recovered, and a small amount of polymolybdate (colorless white solid) and three pieces of yellow plates (**1**) were formed. For **1**, yield 0.05 mg (0.05%).

$(PPh_4)_2[\{W^{VI}O_2(bdt)\}_2(\mu\text{-}O)]$ (3). DMF solution (4 cm^3) of $(PPh_4)[W^{V}O(bdt)_2]$[3c] (**4**) (166 mg, 0.27 mmol) was prepared under Ar atmosphere. On this solution, hexane (4 cm^3) and diethyl ether (4 cm^3) was layered, successively. Then this system was placed at 3 °C for 30 d to precipitate crystals. During the crystal formation, a small amount of air was introduced through a small opening of the glass plug. Finally, 20 mg of **4** was recovered, and small amount of polytungstate (colorless white solid) and dark yellow plates (**3**) were formed. For **3**, yield 3 mg (2×10^{-3} mmol). ^{1}H NMR (DMSO-d_6) δ = 7.96 (t, 8H, PPh_4^+), 7.8 (m, 32H, PPh_4^+), 7.11 (q, 4H, J = 3.4, 5.9 Hz, H(2,6) of bdt), 6.78 (q, 4H, J = 3.3, 5.8 Hz, H(3,4) of bdt).

$(NEt_4)_2[\{W^{VI}O_2(ndt)\}_2(\mu\text{-}O)]$ (5). DMF solution (15 cm^3) of $(NEt_4)[W^{V}O(ndt)_2]$[3g] (**6**) (520 mg, 0.73 mmol) was prepared under Ar atmosphere. On this solution, hexane (20 cm^3) and diethyl ether (50 cm^3) was layered, successively. Then this system was placed at 3 °C for 30 d to precipitate crystals. During the crystal formation, a small amount of air was introduced through a small opening of the glass plug. Finally, 100 mg of **6** was recovered, and small amounts of polytungstate (colorless white solid) and dark brown plates (**5**) were formed. For **5**, yield 3 mg (3×10^{-3} mmol). ^{1}H NMR (DMSO-d_6) δ = 7.67 (s, 4H, H(1,4) of ndt), 7.62 (q, 4H, J = 3.1, 6.1 Hz, H(5,8) of ndt), 7.23 (q, 4H, J = 3.2, 6.1 Hz, H(7,6) of ndt), 3.20 (q, 16H, NEt_4^+), 1.16 (tt, 24H, NEt_4^+).

Physical Measurements. All spectra except ^{1}H NMR were taken at room temperature (25±2°C). The absorption spectra were recorded on a Shimadzu UV3100-PC using a 1 mm cell and 1 mmol dm^{-3} DMSO-d_6 solution under argon atmosphere. The extinction coefficients are given in $M^{-1}\,cm^{-1}$ (1 M = 1 mol dm^{-3}). Raman and IR spectra were taken on a JASCO NR-1800 spectrophotometer with a 514.5 and 632.8 nm excitation line and on a JASCO FT/IR-8300 spectrophotometer, respectively. The cyclic voltammograms were measured on a BAS 100W with a three-electrode system consisting of a glassy carbon working electrode, a platinum-wire auxiliary electrode, and a saturated calomel compartment. The sample concentration was 1 mmol dm^{-3} in DMSO-d_6 and a solution of tetra-*n*-butylammonium perchlorate (0.1 M) was employed as a supporting electrolyte.

Reaction of 5 with Benzoin. The reaction systems containing **5** and benzoin were monitored using a 270 MHz ^{1}H NMR spectrometer (JEOL EX-270) with measurements of the ^{1}H signals of benzoin, benzil, and naphthalenedithiolate of **5**. An NMR tube containing DMSO-d_6 (0.69 cm^3), **5** (0.75 mg, 0.69×10^{-3} mmol) and benzoin (0.25 mg, 1.2×10^{-3} mmol) was prepared and the contents were quickly mixed by shaking at 35 °C. The ^{1}H NMR spectra were taken after 0, 25, 40, 84, 128, and 177 h. NEt_4^+ signals were used as an internal standard for this reaction. The benzoin–OH and α-CH signals (6.00 and 6.03 ppm in DMSO-d_6, respectively) were assigned from the α-C-deuterated benzoin.[9]

Catalytic Air Oxidation of Benzoin with 5. To DMSO-d_6 (0.66 cm^3) was added **5** (0.36 mg, 0.33×10^{-3} mmol) and benzoin (1.31 mg, 6.22×10^{-3} mmol) under argon atmosphere. Soon after making the solution, the reaction was started with the bubbling of air (30 s) in an NMR tube. The system was monitored using a 400 MHz ^{1}H NMR spectrometer (JEOL GSX-400) with measurements of the ^{1}H signals of benzoin and benzil at 35 °C. The naphthalenedithiolate signals of **5** were not observed due to the overlapping of benzoin signals. The ^{1}H NMR spectra were taken until 80 h.

Crystallographic Data Collections and Data Reduction for 1, 3, and 5. Crystals of **1** (brown plate), **3** (yellow plate), and **5** (brown plate) was mounted in a glass capillary under argon atmosphere. All measurements were made on a Rigaku AFC-5R or -7R diffractometer with graphite monochromated Mo $K\alpha$ radiation and a 12 kW rotating anode generator. Cell constants and an orientation matrix for data collection, obtained from a least square refinement using the setting angle of 25 carefully centered reflections in the 2θ range of 15—20°, 20—23°, and 25—27° for **1**, **3**, and **5**, respectively, corresponded to a monoclinic cell with dimensions listed in Table 1. Based on the systematic absences, the successful solutions and refinement of the structures, the space group were determined to be $P\bar{1}$ (#2), *Pbca* (#61), and *Pbcn* (#60) for **1**, **3**, and **5**, respectively. The data were collected at 23 °C using the ω scan technique to a maximum 2θ value of 60°. Of the 10949 (11311 unique), 8801, and 6623 reflections for **1**, **3**, and **5**, respectively, were collected. The intensities of three representative reflections, measured after every 150 reflections, were shown without any significant change. The linear absorption coefficient for Mo $K\alpha$ is 5.63, 44.33, and 58.70 cm^{-1} for **1**, **3**, and **5**, respectively. An empirical absorption correction, based on azimuthal scans of three reflections, was applied, which resulted in transmission factors ranging 0.88—1.00, 0.55—1.00, and 0.83—1.00 for **1**, **3**, and **5**, respectively. The data were corrected for Lorentz and polarization effects.

Structure Solution of 1, 3, and 5, and the Refinement. The structure was solved by the direct method. The non-hydrogen atoms were refined anisotropically. Hydrogen atom coordinates were included at idealized positions with an assumed C–H distance of 1.08 Å and the hydrogen atoms were given with the same temperature factor as that of carbon atom to which they were bonded. The final cycles of least-squares refinement were based on 3772, 2705, and 3553 for **1**, **3**, and **5**, respectively, observed reflections ($I > 3.00\sigma(I)$), and 398, 330, and 223 variable parameters for **1**, **3**, and **5**, respectively, and converged with R (R_w) = 0.083 (0.071), 0.044 (0.043), and 0.041 (0.029) for **1**, **3**, and **5**, respectively.

Neutral atom scattering factors were taken from Ref. 10. Anomalous dispersion effects were included in F_{calc}; the values for $\Delta f'$ and $\Delta f''$ were taken from Ref. 10. All calculations were performed using the teXsan crystallographic software package of Molecular Structure Corporation.

Results and Discussion

Air Oxidation Study. All $(Mo^{V}O)^{3+}$ thiolate complexes solubilized in DMF, CH_3CN, and DMSO degrade immediately under air atmosphere. For example, when an anaerobically prepared DMF solution (1 mmol dm^{-3}) of $(NEt_4)[Mo^{V}O(Ph_3Si\text{-}bdt)_2]$ (**2**) was exposed to air, the blue solution was changed to very pale yellow within 5 min. This pale yellow color suggests the oxidation of thiolate ligands and the formation of polymolybdate complexes, such as $[Mo^{VI}_6O_{19}]^{2-}$.[11]

As described above, we have reported the air oxidation of benzoin with a $(Mo^{V}O)^{3+}$ thiolato complex. The active species have been considered as an air oxidation product of the $(Mo^{V}O)^{3+}$ complex.[5d] To isolate an air oxidation intermediate, we have examined the reaction of $[M^{V}O(dithiolato)_2]^-$ (M = Mo and W, dithiolato = bdt, Ph_3Si-bdt, and ndt) with a trace amount of air as described in the Experimental section.

Table 1. Crystal and Refinement Data for $(NEt_4)_2[\{Mo^{VI}O_2(Ph_3Si\text{-}bdt)\}_2(\mu\text{-}O)]\cdot 2DMF$ (**1**), $(PPh_4)_2[\{W^{VI}O_2(bdt)\}_2(\mu\text{-}O)]$ (**3**), and $(NEt_4)_2[\{W^{VI}O_2(ndt)\}_2(\mu\text{-}O)]$ (**5**)

	1	**3**	**5**
Chemical formula	$C_{70}H_{90}O_7N_4Mo_2S_4Si_2$	$C_{60}H_{48}O_5P_2W_2S_4$	$C_{36}H_{52}O_5N_2W_2S_4$
Mw	1475.79	1406.92	1088.76
Cryst syst	Triclinic	Orthorhombic	Orthorhombic
Color	Brown	Yellow	Brown
Cryst shape	Plate	Plate	Plate
Space group	$P\bar{1}$ (#2)	*Pbcn* (#60)	*Pbca* (#61)
a/Å	9.73(1)	20.926(6)	15.885(3)
b/Å	21.47(4)	17.306(5)	24.729(3)
c/Å	9.12(2)	15.224(4)	10.415(3)
α/deg	100.8(2)		
β/deg	109.8(1)		
γ/deg	88.0(1)		
V/Å^3	1759(5)	5513(4)	4091(1)
Z	1	4	4
d_{calcd}/g cm^{-3}	1.393	1.695	1.767
Radiation	Mo $K\alpha$	Mo $K\alpha$	Mo $K\alpha$
μ(Mo $K\alpha$)/cm^{-1}	5.63	44.33	58.70
Temp/°C	23	23	23
Scan speed/deg min^{-1}	8	6	6
2θ range/deg	6—60	6—60	6—60
Octants	$\pm h, \pm k, \pm l$	$+h, +k, +l$	$+h, +k, +l$
No. of reflections			
(total)	10949	8801	6623
(unique)	10381 (R_{int}=0.066)	8801	6623
No. of used data ($I_0>3\sigma(I)$)	3772	2705	3553
R	0.083	0.044	0.041
R_w	0.071	0.043	0.029
GOF	2.93	1.28	2.54

From the reaction, the mono(dithiolato) complexes which has $[\{M^{VI}O_2\}_2(\mu\text{-}O)]^{2+}$ (M = Mo and W) structure, **1**, **3**, and **5**, were isolated and characterized by X-ray crystallography.

Both NEt_4^+ and PPh_4^+ cations were used for the isolation of $[\{M^{VI}O_2\}_2(\mu\text{-}O)]^{2+}$ (M = Mo and W) complexes. As a result, only **1** (NEt_4^+), **3** (PPh_4^+), and **5** (PPh_4^+) were isolated successfully. In each structure, the corresponding counter ions were probably suitable for crystallization.

A proposed air oxidation pathway is shown in Fig. 1. Initially, two molecules of $[M^{V}O(SR)_4]^-$ (M = Mo and W) are oxidized into a binuclear complex, $[\{M^{VI}O_2(SR)_2\}_2(\mu\text{-}O)]^{2-}$ accompanying the oxidation and/or dissociation of two thiolate ligands. Then, by the further oxidation at the thiolate ligand, polyoxometallate is formed.

In the case of Mo, we can isolate a binuclear state only from the Ph_3Si-bdt complex, **2**. In this case, the bulkiness of the Ph_3Si-bdt ligand retards continued oxidation of **2** and **1** into polymolybdate.

Crystal Structures. Figures 2, 3, and 4 show the ORTEP drawings of the anion part of the crystal structures of **1**, **3**, and **5**, respectively. In Table 1, crystal and refinement data are listed. Tables 2 and 3 and Fig. 5 show the selected bond angles and bond lengths to compare them with related complexes. For **1**, because of the weakness of the reflections especially above $2\theta > 40°$, only 3772 of 10949

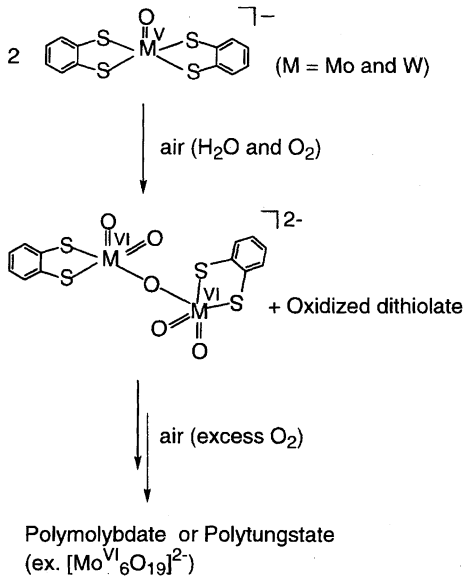

Fig. 1. Air oxidation pathway of $[W^{V}O(dithiolato)_2]^-$ complexes.

reflections were observed ($I > 3.00\sigma(I)$). Those weak reflections probably result in high R (R_w) values. No disorder problem associated with Et_4N^+ cations (in **1** and **5**) and DMF (in **5**) was observed. In all cases of **1**, **3**, and **5**, two cations,

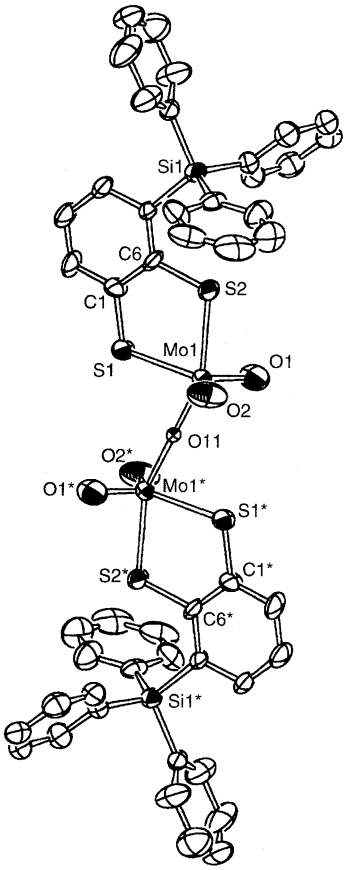

Fig. 2. The ORTEP drawing of anion part of $(NEt_4)_2[\{Mo^{VI}O_2(Ph_3Si\text{-}bdt)\}_2(\mu\text{-}O)]\cdot 2DMF$ (**1**).

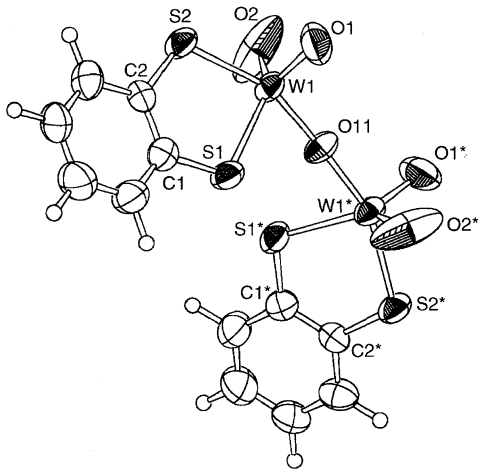

Fig. 3. The ORTEP drawing of anion part of $(PPh_4)_2[\{W^{VI}O_2(bdt)\}_2(\mu\text{-}O)]$ (**3**).

the complex anion and crystallized solvent molecules (DMF in **5**) were well separated from each other. Each $M^{VI}O_3S_2$ (M = Mo and W) core has approximately trigonal bipyramidal geometry with *cis*-di(terminal oxo), one bridged oxo, and one dithiolate ligand. Those complexes are the first examples of mono(dithiolene) coordination to the $(M^{VI}O_2)^{2+}$ (M = Mo and W) structure. In each case of **1**, **3**, and **5**, the bridged atom, O11, is an inversion center crystallographically. T. Shibahara,[12a] F. A. Cotton,[12b] and K. Wieghardt[12c] have reported similar binuclear complexes with non-thiolate ligands, $[\{Mo^{VI}O_2(dmso)_2(NCS)\}_2(\mu\text{-}O)]$ (**7**), $[\{Mo^{VI}O_2(oxalate)(H_2O)\}_2(\mu\text{-}O)]$ (**8**), and $[\{Mo^{VI}O_2(1,4,7\text{-trimethyl-}1,4,7\text{-triazacyclononane})\}_2(\mu\text{-}O)]$, respectively.

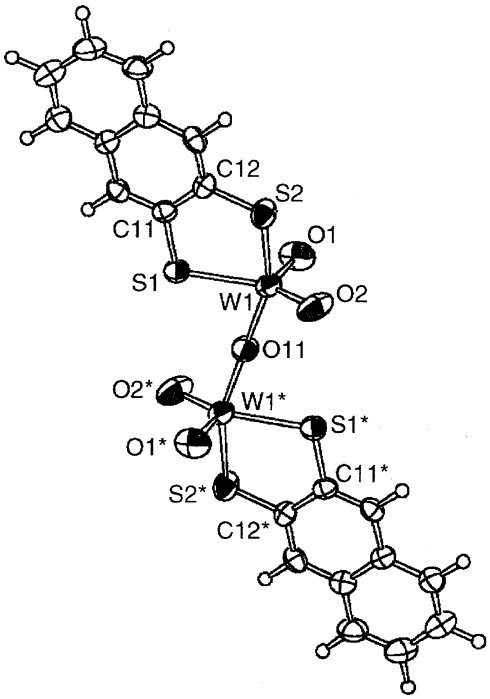

Fig. 4. The ORTEP drawing of anion part of $(NEt_4)_2[\{W^{VI}O_2(ndt)\}_2(\mu\text{-}O)]$ (**5**).

Table 2. Comparison of Structural Dimensions (Å and deg) for $(NEt_4)_2[\{Mo^{VI}O_2(Ph_3Si\text{-}bdt)\}_2(\mu\text{-}O)]\cdot 2DMF$ (**1**), $[\{Mo^{VI}O_2(dmso)_2(NCS)\}_2(\mu\text{-}O)]$ (**7**), and $[\{Mo^{VI}O_2(oxalate)(H_2O)\}_2(\mu\text{-}O)]$ (**8**)

	1	**7**	**8**
<O=Mo=O)	113.2(5)	104.6(2)	106(1)
<O–Mo=O)	101.0(3)		
	101.5(3)		
<S1–W=O1)	127.8(4)		
<S1–W=O2)	118.3(4)		
<S2–W=O1)	89.4(3)		
<S2–W=O2)	95.4(3)		
Mo=O	1.651(9)	1.691(5)	1.70(2)
	1.675(9)	1.686(5)	1.68(2)
Mo–O	1.884(9)	1.864(1)	1.876(2)
Ref.	This work	11a	11b

Compared with the values for non-thiolate complexes **7** (104.6(2)°) and **8** (106(1)°), the widening of the O=Mo=O angle was observed in **1** (113.2(5)°). From a theoretical analysis, it is evident that Mo 4d orbital plays a dominant role in stabilizing the bent O=Mo=O angle of ca. 110°.[13] The coordination number of Mo(VI) ion (penta-coordinated) is smaller than those of **7** and **8** (hexa-coordinated). This in turn leads to the O=Mo=O angle widening in **1** to minimize their orbital energy. The same rationale also can apply to the difference of O=W=O angles between mono(dithiolato)

Table 3. Comparison of Structural Dimensions (Å and deg) for $(PPh_4)_2[\{W^{VI}O_2(bdt)\}_2(\mu\text{-}O)]$ (**3**), $(NEt_4)_2[\{W^{VI}O_2(ndt)\}_2(\mu\text{-}O)]$ (**5**), $(PPh_4)_2[W^{VI}O_2(bdt)_2]$ (**9a**), and $(NEt_4)_2[W^{VI}O_2(ndt)_2]\cdot H_2O$ (**10**)

	3	**5**	**9a**	**10**
<O=W=O)	106.0(6)	107.8(3)	102.6(3)	102.0(1)
<O–W=O)	100.9(4)	105.0(2)		
	102.3(4)	99.9(2)		
<S1–W=O1)	117.0(4)	111.2(2)		
<S1–W=O2)	136.2(5)	139.8(2)		
<S2–W=O1)	94.3(3)	99.4(2)		
<S2–W=O2)	88.7(4)	84.7(2)		
W=O	1.69(1)	1.704(5)	1.727(6)	1.744(2)
	1.731(9)	1.729(4)	1.737(6)	1.750(2)
W–O	1.8899(7)	1.8851(3)		
Ref.	This work	This work	3c	3g

complexes, **3** and **5**, (106.0(6)° and 107.8(3)° for **3** and **5**, respectively) and bis(dithiolato) complexes which have hexacoordinated W(VI) atom, $(PPh_4)_2[W^{VI}O_2(bdt)_2]$[3c] (**9a**) and $(NEt_4)_2[W^{VI}O_2(ndt)_2]\cdot H_2O$[3g] (**10**), (102.6(3)° and 102.0(1)° for **9a** and **10**, respectively).

Of particular interest are the lengths of M^{VI}–S (M = Mo and W) bonds. In the case of bis(dithiolato) complexes, **9a** and **10**, the W–S distances *trans* to the oxo groups (mean values; 2.60(1) Å for **9a** and 2.599(8) Å for **10**) are elongated, compared with those of *cis* to the oxo (mean values; 2.43(1) Å for **9a** and 2.423(6) for **10**). This difference is due to the *trans* influence from the strong π-donor effect by the terminal oxo ligands. On the other hand, in the case of mono(dithiolato) complex, **5**, the W–S bond length are observed as 2.450(4) and 2.440(2) Å. The lengths of observed W–S bonds are at intermediate values between the lengths of W–S *trans* to oxo (mean; 2.599(8) Å) and those of *cis* to oxo (mean; 2.423(6)

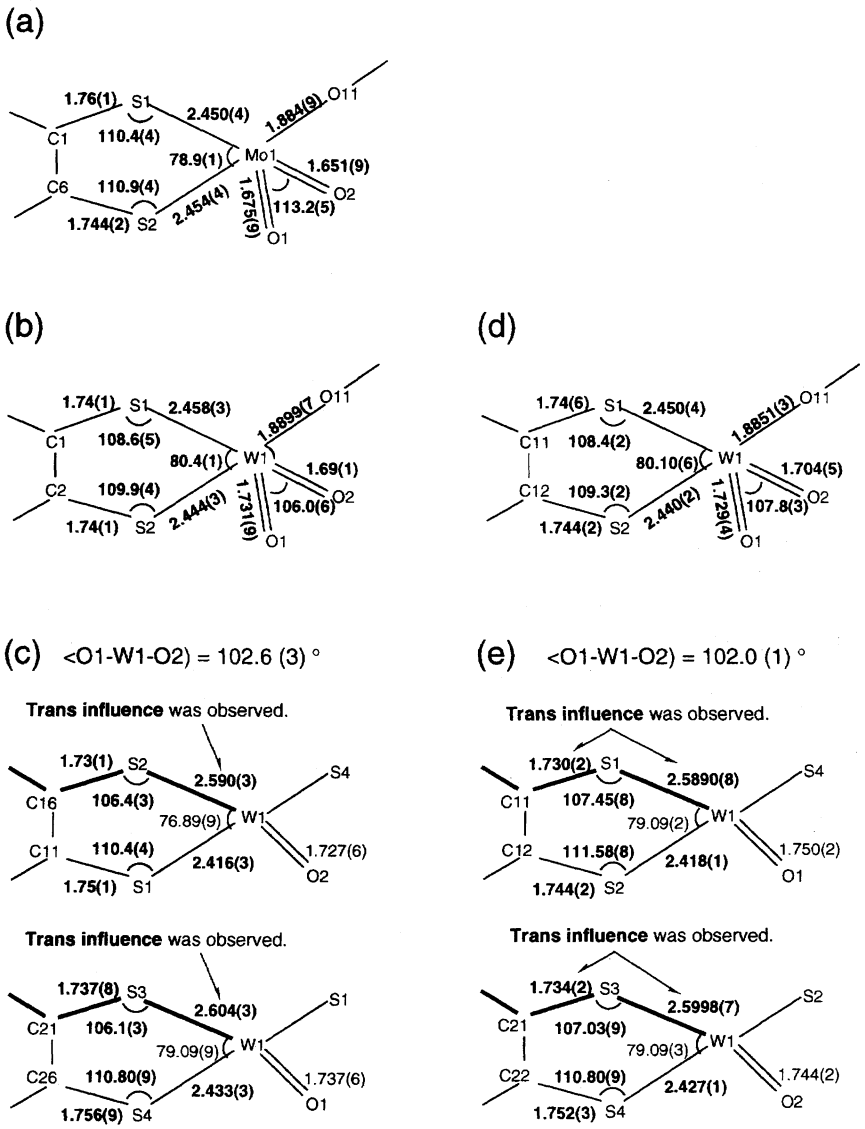

Fig. 5. Selected bond angles (deg) and length (Å) in the sructures of (a) $(NEt_4)_2[\{Mo^{VI}O_2(Ph_3Si\text{-}bdt)\}_2(\mu\text{-}O)]\cdot 2DMF$ (**1**), (b) $(PPh_4)_2[\{W^{VI}O_2(bdt)\}_2(\mu\text{-}O)]$ (**3**), (c) $(NEt_4)_2[\{W^{VI}O_2(ndt)\}_2(\mu\text{-}O)]$ (**5**), (d) $(PPh_4)_2[W^{VI}O_2(bdt)_2]$ (**9a**), and (e) $(NEt_4)_2[W^{VI}O_2(ndt)_2]\cdot H_2O$ (**10**).

Å) as observed in **10**. Particularly the S1–W1 length of **5** (2.450(4) Å) which is placed at *trans* to oxo is slightly longer than that of S2–W1 (2.440(2) Å). Thus in the case of mono-(dithiolato) structure, $[\{W^{VI}O_2(\text{dithiolato})\}_2(\mu\text{-O})]^{2-}$, we did not observe significant labilizing effect among the strong π-donors, terminal oxo and thiolate ligands.

UV/vis Absorption Spectra. The UV/vis absorption spectra are shown in Fig. 6. Shoulders were observed in the range, 300—400 nm for **3** and **5** in DMSO-d_6 solution. The absorptions are mainly come from the O→W(VI) and S→W-(VI) LMCT bands since W(VI) ion has d^0 configuration. The ndt complex, **5**, shows a different shape of absorption compared with **3**. This is due to the overlapping of ndt π→π* absorption onto the LMCT band region similar to the case of bis(dithiolato) complexes.[3g]

Raman Spectra. Figure 7 shows the resonance Raman (= RR) spectra of **3** and **5** in the single crystal state with 514.5 and 632.8 nm excitation, respectively. Table 4 lists the RR and IR bands of **3**, **5**, $(NEt_4)_2[W^{VI}O_2(bdt)_2]$ (**9b**), and **10**.[3h] One intense RR band was observed at around 950 cm^{-1} which is assignable to $\nu_s(W^{VI}{=}O)$ stretching. Due to the *cis*-$(W^{VI}O_2)^{2+}$ structure, a weak $\nu_{as}(W^{VI}{=}O)$ band is expected, but we can not detect it in either RR spectra. The IR band of **3** at 894 cm^{-1} is probably $\nu_{as}(W^{VI}{=}O)$ stretching.

The $\nu_s(W^{VI}{=}O)$ bands of the mono(dithiolato) complexes (953 and 946 cm^{-1} for **3** and **5**, respectively) appear in a quite higher wavenumber region compared with those of the bis(dithiolato) complexes (885 and 883 cm^{-1} for **9b** and **10**, respectively). From the comparison of RR spectra, we can expect the weak activation feature of oxo ligands in the $[\{W^{VI}O_2(\text{dithiolato})\}_2(\mu\text{-O})]^{2-}$ structures, **3** and **5**.

In the region, 300—400 cm^{-1}, only weak RR bands were observed. These bands are associated with the vibrations of W–S and W–(μ-O) stretchings.[3h,14]

Electrochemical Properties. Cyclic voltammograms (Fig. 8) in DMSO-d_6 solutions of **3** and **5** exhibit irreversible reduction peaks at −0.86 and −0.85 V vs. SCE respectively. The voltammograms are very similar to those of bis(dithiolato) compounds, **9b** and **10**, which show one pair of irreversible reduction and oxidation peaks (Table 4).[3c,3g] Therefore we can assign those peaks observed for **3** and **5** as the W(VI)/W(V) redox process and the successive O-atom releasing reactions.[3d,15] The ndt complex, **5**, shows almost the same potential at the reduction peak as the bdt complex, **3**, does. Compared with the mono(dithiolene) compounds, **3** and **5**, the potential difference was observed in the case of bis(dithiolato) compounds, **9b** and **10** (−1.26 and −1.41 V vs. SCE, respectively).

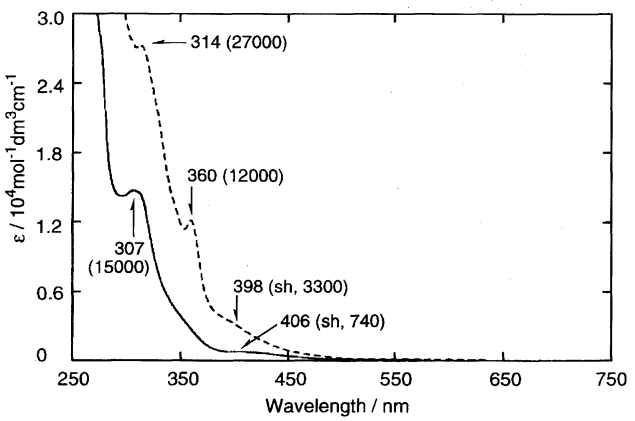

Fig. 6. UV/vis spectra of $(PPh_4)_2[\{W^{VI}O_2(bdt)\}_2(\mu\text{-O})]$ (**3**) (—) and $(NEt_4)_2[\{W^{VI}O_2(ndt)\}_2(\mu\text{-O})]$ (**5**) (- - -) in DMSO-d_6.

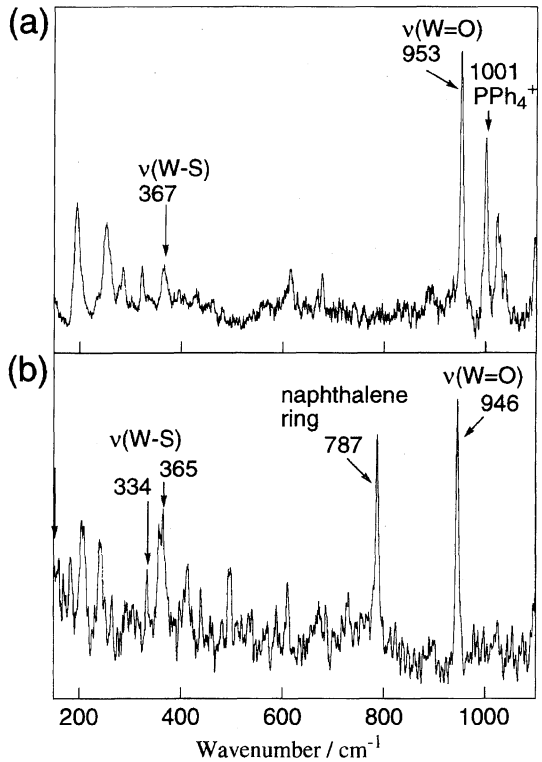

Fig. 7. Raman spectra of $[\{W^{VI}O_2(\text{dithiolato})\}_2(\mu\text{-O})]^{2-}$ complexes. Single crystals were used. (a) $(PPh_4)_2[\{W^{VI}O_2(bdt)\}_2(\mu\text{-O})]$ (**3**) (514.5 nm excitation, 20 mW laser power, 5 cm^{-1} slit width, and 0.5-s dwell time/0.5 cm^{-1} step). (b) $(NEt_4)_2[\{W^{VI}O_2(ndt)\}_2(\mu\text{-O})]$ (**5**) (632.8 nm excitation, 15 mW laser power, 5 cm^{-1} slit width, and 0.5-s dwell time/0.5 cm^{-1} step).

Benzoin Oxidation under Argon Atmosphere. The O-atom donating reactivity of the binuclear mono(dithiolene) complex is of great interest owing to the structural relevance to the enzyme active site. The reaction was examined between the ndt tungsten(VI) complex, **5**, ($[\mathbf{5}]_0 = 1.0$ mmol dm^{-3}) and benzoin ($[\text{benzoin}]_0 = 1.7$ mmol dm^{-3}) in DMSO-d_6 at 35 °C. ^{1}H NMR spectra were used to monitor the system at 0, 25, 40, 84, 128, and 177 h after the reaction. At the same time, a control reaction was examined and this revealed that DMSO-d_6 alone does not oxidize benzoin. Initially the color of the sample was very pale yellow. After 40 h, the color was changed to yellow. The yellow color suggests that the formation of benzil and/or unidentified compounds.

Figure 9 shows the ^{1}H NMR spectral changes until 177 h. From ^{1}H NMR signals, time-conversion curves are plotted for the concentration of benzoin and benzil (Fig. 10). Initially, benzoin and ndt ligand signals of **5** were observed at

Table 4. Raman (IR) Bands of ν(W=O) and ν(W–S), UV/vis Absorption Maxima,[a] and Redox Potential of, $(PPh_4)_2[\{W^{VI}O_2(bdt)\}_2(\mu\text{-}O)]$ (**3**), $(NEt_4)_2[\{W^{VI}O_2(ndt)\}_2(\mu\text{-}O)]$ (**5**), $(NEt_4)_2[W^{VI}O_2(bdt)_2]$ (**9b**), and $(NEt_4)_2[W^{VI}O_2(ndt)_2]\cdot H_2O$ (**10**)

	Raman (IR) band solid state (cm^{-1}) ν(W=O)	ν(W–S) or ν(W–O)	UV/vis absorption in DMF (nm ($mmol^{-1}$ dm^3cm^{-1}) λ_{max} (ε)	Redox potential in DMF (V vs. SCE)
3	953 (954) (ν_s)	367	307 (15000)	−0.86
	(894) (ν_{as})	323	406 (sh, 740)	+0.17
				(Irreversible)
9a	885 (888) (ν_s)	370	323 (sh, 15000)	−1.26
	843 (847) (ν_{as})	352	419 (2300)	+0.14
		326	483 (1300)	(Irreversible)
5	946 (ν_s)	365	314 (27000)	−0.85
		334	360 (12000)	+0.26
			398 (sh, 3300)	(Irreversible)
10	883 (884) (ν_s)	368	391 (sh, 20000)	−1.41
	832 (835) (ν_{as})	357	437 (sh, 10000)	+0.21
		339	475 (sh, 3700)	(Irreversible)

a) The shoulders of absroption bands were determined by the fourth derivatives of the spectrum.

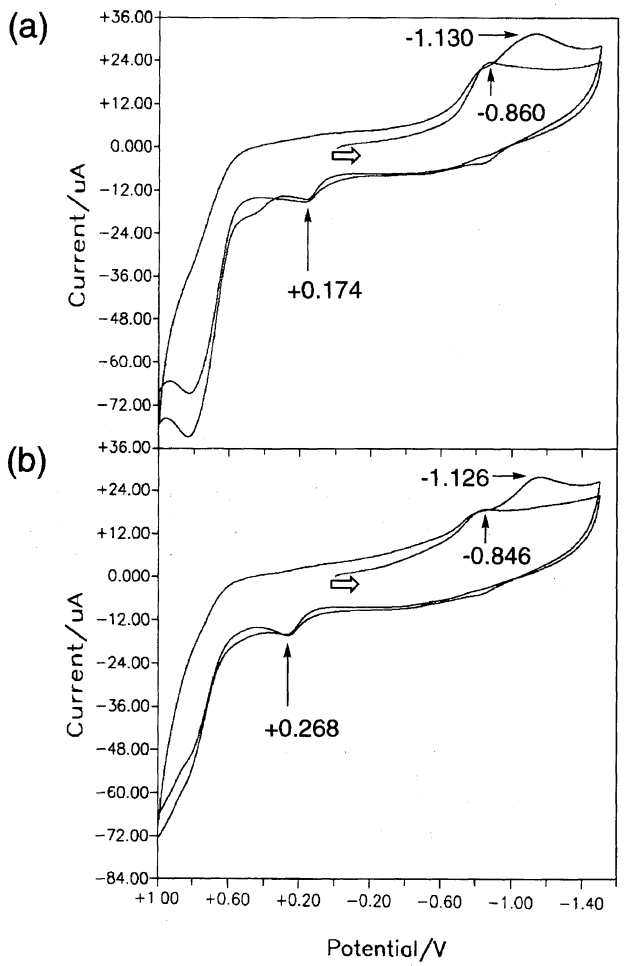

Fig. 8. Cyclic voltammograms of $(PPh_4)_2[\{W^{VI}O_2(bdt)\}_2(\mu\text{-}O)]$ (**3**) and $(NEt_4)_2[\{W^{VI}O_2(ndt)\}_2(\mu\text{-}O)]$ (**5**) in DMSO-d_6. Potential were recorded with a SCE reference electrode. [complex] = 1 mmol dm^{-3}, [n-Bu_4NClO_4] = 0.1 M, and the scan rate: 100 mV s^{-1}.

6.00, 6.03, 7.2—7.6, and 7.96 ppm which come from benzoin α-CH, OH, H(2-6), and H(2′, 3′,5′,6′) of Ph, and H(4′) of Ph, and at 7.23, 7.62, and 7.67 ppm which come from ndt ligand H(6,7), H(5,8), and H(1,4). For the spectra after 25 h and 40 h, a quartet (7.05 ppm) and a broad signal (6.90 ppm) and benzil proton signals (7.92, 7.80, and 7.63) ppm newly appeared. The signals of 7.05 and 6.90 ppm are assignable to the protons (H(6,7) and H(5,8)) of ndt ligand, which probably coordinates to a tungsten ion derived from the reaction of **5** and benzoin. Through the time course, about 1 mmol dm^{-3} of benzoin was consumed. Thus, the reaction proceeds as an equimolar reaction where one molecule of the binuclear complex, **5**, oxidizes one molecule of benzoin under Ar atmosphere.

As shown in Fig. 10, the concentration of benzoin decreased steeply (−0.017 mmol h^{-1}) during the initial 40 h. After 40 h, benzoin was consumed slowly (−0.017 mmol h^{-1}). On the other hand, for 7.05 and 6.90 ppm signals, the integral values were increased with rate constants, 0.018 and 0.024 mmol-of-ndt-ligand/h (during 0—40 h), respectively, and < 0.001 and 0.001 mmol-of-ndt-ligand/h (during 40—177 h), respectively. Therefore, the molar consumption rate of bezoin is almost the same as the molar formation rate of a newly appeared ndt compound. If the newly appeared ndt compound was a ndt-tungsten complex, the new ndt compound should be a product from the benzoin oxidation with **5**. This new complex can be described as $[\{W^{VI}O_2(ndt)\}(\mu\text{-}O)\{W^{IV}O(benzil)(ndt)\}]^{2-}$.

Interestingly, the yield of benzil does not correspond to the molar amount of consumed benzoin, although the reaction was clean and no other product was observed. At all times in the spectra, the amount of benzil (at 40 h, 0.15 mmol dm^{-3}) was lower than that of consumed benzoin (at 40 h, 0.73 mmol dm^{-3}). This difference indicates the existence of a reaction intermediate which is made from benzoin and

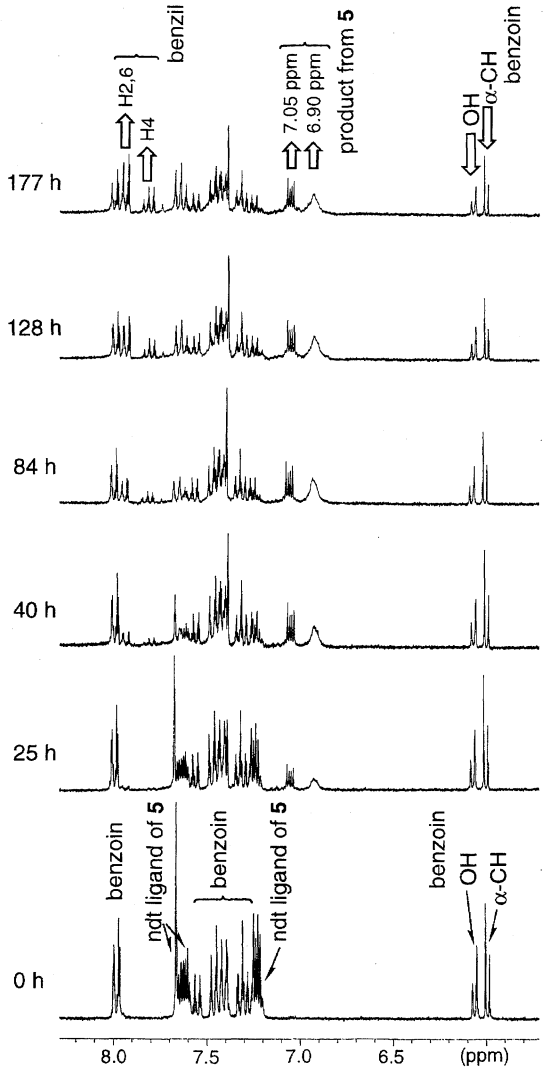

Fig. 9. ^{1}H NMR spectral changes in the reaction of $(NEt_4)_2[\{W^{VI}O_2(ndt)\}_2(\mu\text{-}O)]$ (**5**) with 1.7 equiv of benzoin in DMSO-d_6. Spectral intensity was normalized with the internal standard of NEt_4 signals. The sample was reacted at 35 °C. The spectra were recorded at 30 °C.

5, although the intermediate was not detected in the ^{1}H NMR spectra probably due to its paramagnetic nature from the presence of a W(V) ion. Thus, the benzoin oxidation proceeds in two steps. The formation of a reaction intermediate was also proposed for the benzoin oxidation by Ni(II) acetate[16] and Fe(II) thiolate complexes.[17]

A proposed reaction pathway is shown in Eqs. 3 and 4.

$$[\{W^{VI}O_2(ndt)\}_2(\mu\text{-}O)]^{2-} + \text{benzoin} \longrightarrow [\{W^{VI}O_2(ndt)\}(\mu\text{-}O)\{W^{VI}O_2(\text{benzoin})(ndt)\}]^{2-} \quad (3)$$

$$[\{W^{VI}O_2(ndt)\}(\mu\text{-}O)\{W^{VI}O_2(\text{benzoin})(ndt)\}]^{2-} \longrightarrow [\{W^{VI}O_2(ndt)\}(\mu\text{-}O)\{W^{IV}O(ndt)\}]^{2-} + \text{benzil} + H_2O \quad (4)$$

The benzoin coordination makes a complex which is a probable intermediate, e.g. $[\{W^{VI}O_2(ndt)\}(\mu\text{-}O)\{W^{VI}O_2\text{-}(benzoin)(ndt)\}]^{2-}$. By the oxidation of the coordinated benzoin into benzil, the intermediate complex gives an H_2O molecule and a reduced ndt complex which has a mono-oxotungsten(IV) moiety, e.g. $[\{W^{VI}O_2(ndt)\}(\mu\text{-}O)\{W^{IV}O\text{-}(ndt)\}]^{2-}$. A similar oxidation mechanism could be operating when the molybdenum and tungsten enzymes catalyze

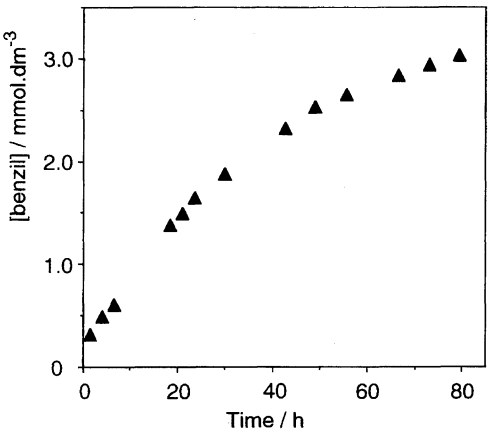

Fig. 11. Time dependence for the catalytic air oxidation of benzoin in the presence of $(NEt_4)_2[\{W^{VI}O_2(ndt)\}_2(\mu\text{-}O)]$ (**5**). Conditions; $[benzoin]_0 = 9.4$ mmol dm^{-3}, [**5**] = 0.5 mM in DMSO-d_6 at 35 °C.

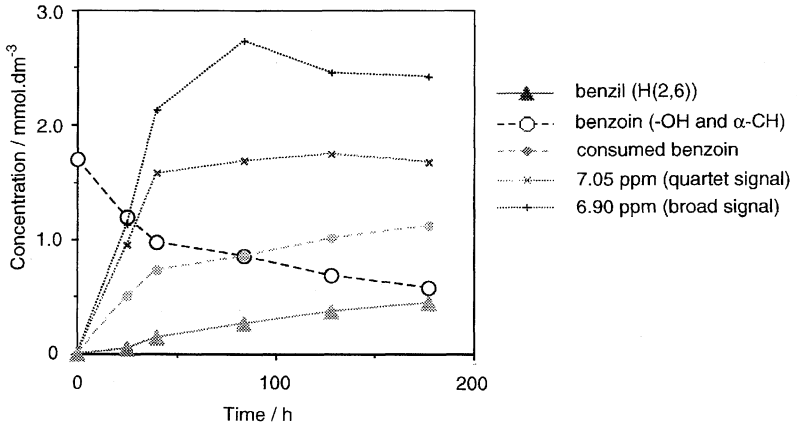

Fig. 10. ^{1}H NMR time-concentration curves in the reaction of $(NEt_4)_2[\{W^{VI}O_2(ndt)\}_2(\mu\text{-}O)]$ (**5**) with 1.7 equiv of benzoin in DMSO-d_6 at 35 °C. For 6.90 and 7.05 ppm signals, the values of proton concentration are plotted.

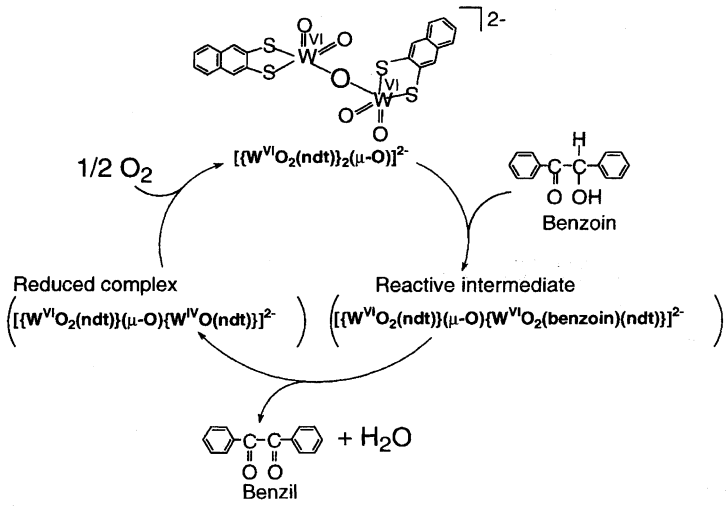

Fig. 12. Proposed catalytic pathway for the air oxidation of bezoin by $(NEt_4)_2[\{W^{VI}O_2(ndt)\}_2(\mu\text{-}O)]$ (**5**).

the reaction with benzoin related substrates.

Catalytic Air Oxidation of Benzoin. Figure 11 shows the time dependence of the catalytic air oxidation of benzoin ($[benzoin]_0 = 9.4$ mmol dm^{-3}) in the presence of **5** ($[\mathbf{5}]_0 =$ 0.5 mmol dm^{-3}). From a control reaction, benzoin was not oxidized by air without the tungsten complex, **5**. The turnover number, 6.1, was achieved at 80 h (calculated from the benzil concentration).

The time-concentration curves were analyzed by pseudo-first order kinetics. At the initial stage (0—24 h, 3.3 turnover), the concentration of benzil strictly followed the equation, $d[benzil]/dt = k_{obs}([benzoin]_0 - [benzil])$ where k_{obs} was 2.00 ($\pm$0.07)$\times 10^{-6}$ s^{-1} (at the 99% confidential).

Our present results indicate a reaction cycle as shown in Fig. 12. The cycle should follow Eqs. 3 and 4. At the final step, the probable reduced complex, $[\{W^{VI}O_2(ndt)\}(\mu\text{-}O)\{W^{IV}O(ndt)\}]^{2-}$, reacts with O_2 to regenerate the starting complex, **5**. Thus, the μ-oxo binuclear species are kept active for further reactions.

Conclusion

During the analysis of the air oxidation product of $(M^VO)^{3+}$ thiolato complexes (M = Mo and W), we have isolated novel mono(dithiolato) coordinated complexes, **1**, **3**, and **5**. The Raman spectra showed that the W^{VI}=O bond in **3** and **5** was not activated in the same way as bis(dithiolato) complexes, **9a** and **10**, due to their mono(dithiolato) coordination. From the reactivity study of **5**, we can conclude that the air oxidation product, $[\{Mo^{VI}O_2(SR)_2\}_2(\mu\text{-}O)]^{2-}$, is a possible active species for the catalytic air oxidation of benzoin with the Mo(V) complex, $[Mo^VO(SR)_4]^-$.

We are grateful for financial supports by JSPS Fellowships (H.O.; No. 1278 (1993—1995), No. 2947 (1995—1997)), and by a Grant-in-Aid for Specially Promoted Research (A.N., No. 06101004) from the Ministry of Education, Science, Sports and Culture.

References

1 a) M. J. Romão, M. Archer, I. Moura, J. J. G. Moura, J. LeGall, R. Engh, M. Schneider, P. Hof, and R. Huber, *Science*, **270**, 331 (1995). b) R. Huber, P. Hof, R. O. Duarte, J. J. G. Moura, I. Moura, M.-Y. Liu, J. LeGall, R. Hille, M. Archer, and M. J. Romão, *Proc. Natl. Acad. Sci. U.S.A.*, **93**, 8846 (1996).

2 a) H. Schindelin, C. Kisker, J. Hilton, K. V. Rajagopalan, and D. C. Rees, *Science*, **272**, 1615 (1996). b) F. Schneider, J. Löwe, R. Huber, H. Schindelin, C. Kisker, and J. Knäblein, *J. Mol. Biol.*, **263**, 53 (1996).

3 a) H. Oku, N. Ueyama, A. Nakamura, Y. Kai, and N. Kanehisa, *Chem. Lett.*, **1994**, 607. b) H. Oku, N. Ueyama, M. Kondo, and A. Nakamura, *Inorg. Chem.*, **33**, 209 (1994). c) N. Ueyama, H. Oku, and A. Nakamura, *J. Am. Chem. Soc.*, **114**, 7310 (1992). d) N. Ueyama, H. Oku, M. Kondo, T. Okamura, N. Yoshinaga, and A. Nakamura, *Inorg. Chem.*, **35**, 643 (1996). e) N. Yoshinaga, N. Ueyama, T. Okamura, and A. Nakamura, *Chem. Lett.*, **1990**, 1655. f) H. Oku, N. Ueyama, and A. Nakamura, *Chem. Lett.*, **1995**, 621. g) H. Oku, N. Ueyama, and A. Nakamura, *Bull. Chem. Soc. Jpn.*, **69**, 3139 (1996). h) H. Oku, N. Ueyama, and A. Nakamura, *Inorg. Chem.*, **34**, 3667 (1995).

4 a) S. K. Das, D. Biswas, R. Maiti, and S. Sarkar, *J. Am. Chem. Soc.*, **118**, 1387 (1996). b) S. K. Das, P. K. Chaudhury, D. Biswas, and S. Sarkar, *J. Am. Chem. Soc.*, **116**, 9061 (1994). c) D. Coucouvanis, A. Hadjikyriacou, A. Toupadakis, S. Koo, O. Ileperuma, M. Draganjac, and A. Salifoglou, *Inorg. Chem.*, **30**, 754 (1991). d) I. K. Dhawan, A. Pacheco, and J. H. Enemark, *J. Am. Chem. Soc.*, **116**, 7911 (1994). e) J. A. McCleverty, J. Locke, B. Ratcliff, and E. J. Wharton, *Inorg. Chim. Acta*, **3**, 283 (1969). f) S. Boyde, S. R. Ellis, C. D. Garner, and W. Clegg, *J. Chem. Soc., Chem. Commun.*, **1986**, 1541. g) R. S. Pilato, K. Eriksen, M. A. Greaney, E. I. Stiefel, S. Goswami, L. Kilpatrick, T. G. Spiro, E. C. Taylor, and A. L. Rheingold, *J. Am. Chem. Soc.*, **113**, 9372 (1991). h) A. A. Eagle, S. M. Harben, E. R. Tiekink, and C. G. Young , *J. Am. Chem. Soc.*, **116**, 9749 (1994). i) I. K. Dhawan and J. H. Enemark, *Inorg. Chem.*, **35**, 4873 (1996). j) E. S. Davies, R. L. Beddoes, D. Collison, A. Dinsmore, A. Docrat, J. A. Joule, C. R. Wilson, and C. D. Garner, *J. Chem. Soc., Dalton Trans.*, **1997**, 3985. k) J. P. Donahue, C. Lorber, E. Nordlander, and R. H. Holm, *J. Am. Chem. Soc.*, **120**, 3259 (1998). l) C. Lorber, J. P. Donahue,

C. A. Goddard, E. Nordlander, and R. H. Holm, *J. Am. Chem. Soc.*, **120**, 8102 (1998). m) J. P. Donahue, C. R. Goldsmith, U. Nadiminti, and R. H. Holm, *J. Am. Chem. Soc.*, **120**, 12869 (1998).

5 a) N. Ueyama, N. Yoshinaga, and A. Nakamura, *J. Chem. Soc., Dalton Trans.*, **1990**, 387. b) H. Oku, N. Ueyama, and A. Nakamura, *Chem. Lett.*, **1996**, 1131. c) N. Ueyama, N. Yoshinaga, T. Okamura, H. Zaima, and A. Nakamura, *J. Mol. Catal.*, **64**, 247 (1991). d) A. Nakamura, N. Ueyama, T. Okamura, T. Zaima, and N. Yoshinaga, *J. Mol. Catal.*, **55**, 276 (1989). e) A. Cervilla, E. Llopis, A. Ribera, A. Dome'nech, and E. Sinn, *J. Chem. Soc., Dalton Trans.*, **1994**, 3511. f) C. Lorber, M. R. Plutino, L. I. Elding, and E. Nordlander, *J. Chem. Soc., Dalton Trans.*, **1997**, 3997.

6 M. K. Chan, S. Mukund, A. Kletzin, M. W. W. Adams, and D. C. Rees, *Science*, **267**, 1463 (1995).

7 T. Trautwein, F. Krauss, F. Lottspeich, and H. Simon, *Eur. J. Biochem.*, **222**, 1025 (1994).

8 a) E. I. Stiefel, in "Molybdenum and Molybdenum-Containing Enzymes," ed by M. Coughlan, Pergamon Press, New York (1980), p. 41. b) J. M. Berg, K. O. Hodgson, S. P. Cramer, J. L. Corbin, A. Elseberry, N. Pariyadath, and E. I. Stiefel, *J. Am. Chem. Soc.*, **101**, 2774 (1979).

9 α-C-deuterated benzoin was prepared by the reported procedure: A. G. Harrison and R. K. M. R. Kallury, *Org. Mass Spectrom.*, **15**, 249 (1980).

10 D. T. Cromer and J. T. Waber, in "International Tables for X-Ray Crystallography," The Kynoch Press, Birmingham, England (1974), Vol. IV, Table 2.2A and Table 2.3.1.

11 M. T. Pope, in "Encyclopedia of Inorganic Chemistry," ed by R. B. King, John Wiley & Sons, Chichester (1994), Vol. 6, p. 3361.

12 a) T. Shibahara, H. Kuroya, S. Ooi, and Y. Mori, *Inorg. Chim. Acta*, **76**, L315 (1983). b) F. A. Cotton, S. M. Morehouse, and J. S. Wood, *Inorg. Chem.*, **3**, 1603 (1964). c) K. S. Bürger, G. Haselhorst, S. Stötzel, T. Weyhermüller, K. Wieghardt, and B. Nuber, *J. Chem. Soc., Dalton Trans.*, **1993**, 1988.

13 K. Tatsumi and R. Hoffman, *Inorg. Chem.*, **19**, 2656 (1980).

14 S. E. Lincolon and T. M. Loehr, *Inorg. Chem.*, **29**, 1907 (1990).

15 L. J. DeHayes, H. C. Faulkner, J. W. H. Doub, and D. T. Sawyer, *Inorg. Chem.*, **14**, 2110 (1975).

16 G. S. Hammond and S. W. Chin-Hua, *J. Am. Chem. Soc.*, **95**, 8215 (1973).

17 W.-Y. Sun, N. Ueyama, and A. Nakamura, *Tetrahedron*, **49**, 1357 (1993).